# Optimized distributive μ-mixing by ‚chaotic' multilamination

F. Schönfeld, K.S. Drese, S. Hardt, V. Hessel, C. Hofmann

Institut für Mikrotechnik Mainz –(IMM),
Carl-Zeiss-Str. 18-20, 55129 Mainz, Germany, schoenfeld@imm-mainz.de

## ABSTRACT

A new micro mixer relying on the consequent utilization of the split-and-recombine (SAR) principle is presented. We show that the mixing can be characterized by a positive finite-time Lyapunov exponent although being highly regular and uniform. Furthermore, a spectral method based on the numerical solution of a pure diffusion equation is developed which allows a computation of concentration profiles and mixing residuals without artifacts from numerical diffusion. Eventually, we compare the performance of the SAR mixer to that of micro mixers relying on interdigital multilamination and hydrodynamic focusing and find it to be superior in terms of mixing efficiency, mixing time and pressure drop in the regime of small Reynolds numbers.

***Keywords***: micro mixing, split-and-recombine principle, spectral method

## 1 INTRODUCTION

Efficient mixing of liquid/liquid systems is one of the paramount tasks in the development of μ-TAS and Lab-on-a-chip systems as well as in micro chemical process engineering. We present a new type of micro mixer relying on a multi-step split-and-recombine (SAR) approach. In the last years, different SAR mixers have been fabricated (see e.g. [1-3]). However, all these mixers were mainly validated experimentally with regard to global process results such as yield, effective reaction times, or properties of produced particles. However, there is, to our best knowledge, neither an in-depth simulation of the mixing efficiency nor an experimental validation of the mixing process itself. Using computational fluid dynamics (CFD), a favorable mixer design was identified which allows for an almost ideal multilamination. The numerical results are corroborated by experimental visualization of multilamination and mixing. Furthermore, a semi-analytical approach is presented allowing for computation of the mixing efficiency. By comparison the mixing performance is found to be superior to that of micro mixers relying on the principle of interdigital multilamination and hydrodynamic focusing [4,5] in the regime of small Reynolds numbers.

## 2 SPLIT-AND-RECOMBINE MIXING

SAR mixing relies on a multi-step procedure. According to its name the basic operations are: splitting of a bi- or multi-layered stream perpendicular to the lamellae orientation into sub-streams and recombination of these. Usually, these basic steps are accomplished by one or more re-shaping steps. The mixing mechanism is schematically displayed in Fig.1.

Figure 1: Schematic of a SAR step: initial configuration, splitting, recombination, reshaping (from left to right).

In the framework of chaotic advection, the mixing performance is commonly characterized by interfacial stretching

$$\lambda(t) = \lim_{L_0 \to 0} L(t) \Big/ L_0 \quad , \tag{1}$$

where $L_0$ and $L(t)$ denote the characteristic dimensions of the interfacial area at $t$=0 and at a finite time $t$, respectively (see e.g. [6,7]). In the case of a 2D, incompressible flow the diffusive mass transport, which determines the mixing performance, depends quadratically on the interfacial stretching λ [6,8]. Chaotic flows ensure particular efficient mixing since they imply an exponential increase of stretching over time. Accordingly, the finite-time Lyapunov exponent σ may be defined via $\lambda(t) \sim e^{\sigma t}$. The repeated application of the SAR principle implies an exponential increase of interfacial area. The corresponding stretching factor is given by

$$\lambda(t) = (2^n - 1) \approx 2^{u \cdot t / l_{SAR}} \quad , \tag{2}$$

where $n$, $u$, and $l_{SAR}$ denote the number of SAR steps, the mean velocity and the length of one SAR unit, respectively. According to Eq. (2) the SAR mixer has a finite-time Lyapunov exponent of $\sigma = \ln 2(u/l)$. Thus, even in case of a highly regular flow pattern a positive finite time Lyapunov exponent can be achieved, a characteristic feature of chaotic advection. Whereas chaotic advection generally induces regions of regular flows and poor mixing

besides regions of high chaoticity where mixing predominantly occurs [6], here, in the case of an ideal SAR multi-lamination, a spatially homogeneous mixing is obtained.

Since the final lamella dimension does not solely depend on the channel width, but also on the number of SAR steps, thorough mixing can be achieved under moderate pressure drops.

## 2.1 CFD-aided layout and validation

The starting point for the layout was the numerical investigation of flow patterns of the so-called caterpillar mixer realized in 1999 [9] which has been successfully applied in various applications (e.g. see [10]). Details on CFD simulations relying on the simultaneous solution of the Navier-Stokes equations and a convection-diffusion equation for a tracer are given in [11]. The CFD model of the revised and optimized geometry is shown in Fig. 2a-c.

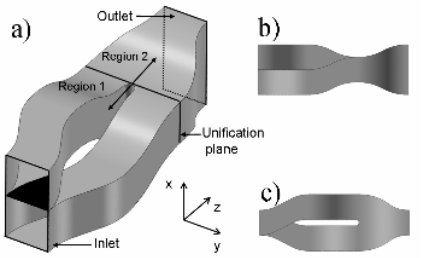


Figure 2: Geometry model of a single mixing step of the optimized SAR mixer - a) slanted view with the splitting layer shown in black; b) side- and c) top-view.

According to the simulation results the developed design leads to an almost prefect lamellae configuration within the SAR mixer for Reynolds numbers below about 30. Thus the mixer is particularly suited for mixing of highly viscous fluids. For higher Reynolds numbers the CFD simulations show more and more deviations from an ideal SAR multi-lamination pattern. Since inertial forces come into play a secondary flow pattern is superposed to the SAR velocity profile of the creeping flow regime.

The good agreement between simulation and experimental results is highlighted in Fig. 3, where the simulated streamline pattern for Re = 0.22 is superimposed to a micrograph of the first SAR step obtained from an iron-rhodanide reaction performed in water/glycerol solutions. Fig. 4 shows a series of micrographs obtained by feeding a transparent and a dyed glycerol/water solution to the mixer. Highly regular lamellae patterns are observed up to the 8$^{th}$ SAR step. The experiments were performed using a SAR mixer realised in PMMA: inlet dimension: 1 mm x 2 mm; length of one SAR unit: 12 mm; number of SAR steps: 8. Fabricational and experimental details are given in [11].

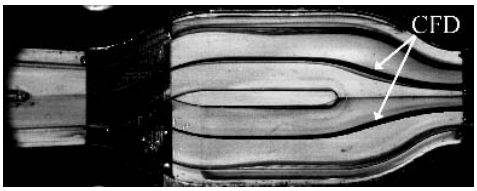


Figure 3: Comparison between CFD results (black lines) and experiment for 85% glycerol/water solutions at a flow rate of 0.2l/h. The black lines denote the numerically computed streamlines seeded at the lamellae interface at the inlet (taken from [11]).

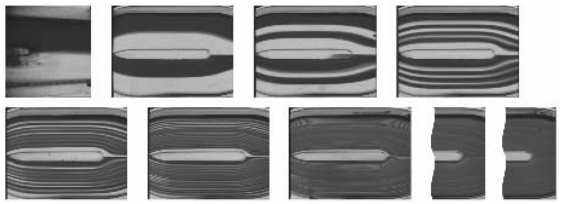

Figure 4: Optical inspection of multi-lamination in the SAR mixer over 8 mixing steps [11]. The dyed (water-blue) and transparent lamellae of a 85% glycerol/water solution are shown in dark and light gray, respectively. The applied total volume flow rate of 0.2 l/h corresponds to Re = 0.22.

## 2.2 Analytical Approach

The CFD simulations allow to study the flow distribution and the arrangement of fluid lamellae. However, even if grids with more than $10^6$ computational cells are used, a solution of the convection-diffusion equation for concentration fields in liquids can hardly be achieved with appropriate accuracy. The reason are discretization errors which induce an artificial diffusive transport [12-14]. A quantity characterizing their magnitude is the cell-based Peclet number, $Pe = u l_c/D$, where $u$ denotes a typical flow velocity, $l_c$ the length scale of a computational cell, and $D$ the molecular diffusivity. As outlined above the SAR mixer is especially suited for mixing of highly viscous liquids. If a liquid of a viscosity of 0.1 Pa·s is assumed, characteristic diffusion constants of the order of $10^{-11}$ m$^2$/s are obtained according to the Stokes-Einstein relation. The length scale of the computational cells is of the order of 50 µm for typical grids. For a Reynolds number of 30 the average flow velocity is approximately 11 cm/s. These numbers imply a cell-based Peclet number of $5.5 \cdot 10^5$, indicating that even on grids with multi-million cells it is usually not possible to compute the mixing performance of the SAR mixer for highly viscous liquids using standard CFD techniques.

In order to approximately compute the time evolution of the concentration field inside the mixer, a method was developed which is based on the numerical solution of a pure diffusion equation using a spectral method. The

method rests on the assumption that the mixing process can be regarded as a diffusive mass transfer in a frame-of-reference co-moving with the average flow velocity. That way the velocity profile inside the mixer is replaced by a plug-flow profile. Furthermore it is assumed that the fluid lamellae are aligned with the x-axis of Fig. 2 and are of equal thickness. Fig. 4 indicates that this assumption is reasonable for low Reynolds numbers although lamellae next to the channel walls are slightly thicker than the lamellae in the middle. In accordance with these approximations, the diffusion equation is solved in a plane perpendicular to the flow being swept through the mixer geometry with the average flow velocity. In order to study the two branches of the mixing step independently, each branch is assigned its own plane. For taking effects of hydrodynamic focusing into account, it is helpful to write down the diffusion equation using a non-dimensionalized spatial variable $s$

$$\frac{\partial c}{\partial t} = \frac{D}{L^2}\frac{\partial^2 c}{\partial s^2} \quad , \tag{3}$$

where $L$ is the channel width and $s = s'/L$, with $s'$ being the spatial coordinate in width direction. At the inlet of a mixing step $s'$ is identical to $y$. When the plane on which the diffusion equation is solved is swept through the mixer geometry, the length scale changes, i.e. $L = L(t)$.

In order to solve the diffusion equation on these planes perpendicular to the flow, the geometry of a mixing step is divided into two regions, as shown in Fig. 2. Region 1 is the region upstream of the unification plane, while region 2 comprises those parts downstream of the unification plane. In both of these regions, the concentration field is expanded in harmonics

$$c_n(s',t) = \frac{1}{2} + \sum_{i=0}^{\infty} a_i^{(n)}(t)\sin k_i s \tag{4}$$

where $n$ = 1, 2 denotes the region where this expansion is applied and the wave numbers $k_i$ are given by $(2i+1)\pi$. Assuming two inlet lamellae entering with identical flow rates with tracer concentrations of 0 and 1, respectively, no cosine functions appear in Eq. 4 due to antisymmetry with respect to inversion of the x-axis. For a given volume flow, the unification plane will be reached after a specific mean residence time $t_u$. The channel width before and after unification of the two streams are $L_- = L(t_u - \varepsilon)$ and $L_+ = L(t_u + \varepsilon)$, where $\varepsilon$ is an infinitesimal number. Obviously, $L_+ = 2L_-$. When entering region 2, the concentration field is composed of two solutions for region 1 shifted by an amount ½ to the left and to the right, respectively. The resulting expression can be cast into the following form

$$c_2(s',t) = \frac{1}{2} + \sum_i a_i^{(1)}(t_u)(-1)^i[\theta(-s_-) - \theta(s_-)]\cos k_i s_- \tag{5}$$

where $\Theta(s)$ denotes the heaviside function and $s_- = s'/L_-$. The goal is now to write the solution in region 2 as an expansion in the Fourier modes of a domain with a width of $L_+$. Again, for reasons of symmetry only the sin-components contribute and the expansion coefficients are given as

$$a_i^{(2)}(t_u) = \frac{2}{L_+}\int_{-L_+/2}^{L_+/2} c_2(s',t)\sin k_i s_+ \, ds' \tag{6}$$

where $s_+ = s'/L_+$. When inserting the expression for $c_2(s',t)$ the integrals involving a product of a sin and a cos function can be computed analytically and straightforward algebra yields

$$a_i^{(2)}(t_u) = \sum_j (-1)^{j+1} a_j^{(1)}(t_u)\frac{k_i}{k_i^2/4 - k_j^2} \tag{7}$$

When inserting this expression into Eq. 4, the concentration field at the entrance to region 2 of the mixing step is obtained. Within each of the two regions, the time evolution of the concentration field is obtained when inserting the series expansion of Eq. 4 into Eq. 3. This way, an ordinary differential equation for the expansion coefficients is obtained which can be solved in a straightforward manner by integration to give

$$a_i^{(n)}(t) = a_i^{(n)}(0)\exp\left(-Dk_i^2\int_0^t \frac{dt'}{L^2(t')}\right) \tag{8}$$

It should be noted that Eq. 8 can only be applied within either region 1 or 2. The transition between the two regions is described by Eq. 7. The translation between the time coordinate appearing in the previous equations and the spatial coordinate along the mixing channel is performed using the mean flow velocity $u$. For the investigation of mixing in the SAR mixer, it is necessary not only to compute the concentration profile in a single mixing step, but rather a sequence of steps has to be considered. The complete algorithm for determining the concentration profile in a multi-step mixer consists of the following steps which have to be performed iteratively:

- Computation of the time evolution of the Fourier coefficients describing the concentration distribution at the inlet of an SAR step via Eq. 8.
- Derivation of the corresponding coefficients in region 2 using Eq. 7.
- Computation of time evolution in region 2 (Eq. 8)
- Translation of the coefficients from the outlet of region 2 to the inlet of region 1.

Figure 5 shows the mixing residual, i.e. the average deviation from perfect mixing, deduced from the concentration profiles at the interface between region 1 and region 2 of Fig. 2. for a diffusion constant of $1.768 \cdot 10^{-11}$ $m^2/s$ and a total flow rate of 0.2 l/h.

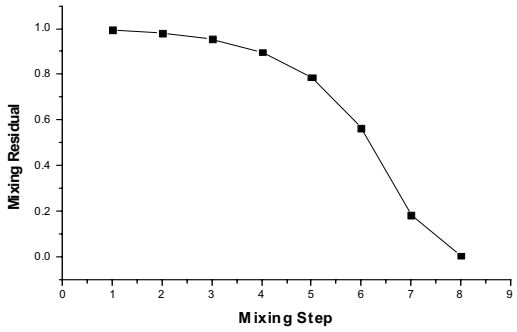


Figure 5: Mixing residual vs. number of SAR steps.

## 3 COMPARISON TO INTERDIGITAL MICRO MIXERS

The generic design of micro mixers relying on interdigital multilamination and hydrodynamic focusing as shown in Fig. 6 was analytically investigated in [5].

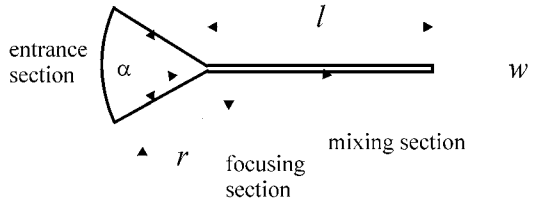


Figure 6: Mixer design analyzed in [5].

The two fluids enter through inlets equally distributed over the entrance section having a pitch *dp* and form an interdigitated lamellae pattern. With the assumptions outlined above concentration profiles are computed by solving Eq. 3 by means of a spectral method. Assuming a mixer geometry which reproduces a mixing residual of 0.007 and a mixing time of about 14 s as found in the case of the SAR mixer after the $8^{th}$ step, one obtains a pressure drop of 0.2 bar in the case of multilamination and hydrodynamic focusing, whereas, a pressure drop of about 0.0038 bar is obtained for the SAR mixer for an highly viscous liquid having a kinematic viscosity $\eta = 80$ mPas.

## 4 SUMMARY ANS CONCLUSION

An improved mixer layout was derived by means of CFD simulations which assures an almost ideal realization of SAR mixing. Generally, a positive finite-time Lyapunov exponent which is a generic feature of chaotic advection is associated with the SAR mixer. The corresponding exponential stretching of interfacial area together with the uniform lamellae distribution ensures efficient homogeneous mixing especially at Reynolds numbers below 30.

The mixing performance was approximately calculated by adapting a spectral method to the particular geometry. The semi-analytical approach allows to overcome problems due to discretization errors as well as the computation of concentration profiles and corresponding mixing residuals. A simulation run takes about 10 s on a standard PC compared to hours which are typically needed for CFD simulations.

Furthermore, in the low-Reynolds-number regime the multi-step nature of the SAR mixing concept leads to a superior mixing performance at equal pressure drop compared to the concept of interdigital multilamination and hydrodynamic focusing.

## REFERENCES


[1] N. Schwesinger, T. Frank and H. Wurmus, J. of Micromech. and Microeng., 1996, 6, 99.

[2] J.P. Branebjerg, J., Gravesen, J.P. Krog and C.R. Nielsen, IEEE-MEMS '96, USA, 1996, 441.

[3] H. Mensinger, T. Richter, V. Hessel, J. Döpper and W. Ehrfeld, in Micro Total Analysis System, A. van den Berg, P. Bergfeld (Eds.), Kluwer Academic Publishers, Dordrecht 1995, 237.

[4] V. Hessel, S. Hardt, H. Löwe and F. Schönfeld, AIChE J., 2003, 49, 566.

[5] K.S. Drese, IMRET 7, Chem. Eng. J., accepted.

[6] J.M. Ottino, F.J. Muzzio, M. Tjahjadi, J.G. Franjione, S.C. Jana and H.A. Kusch, Science, 1992, 257, 754.

[7] D.R. Sawyers, M. Sen and H.-C. Chang, Chem. Eng. J., 1996, 64, 129.

[8] J.M. Ottino, "The Kinematics of Mixing: Stretching, Chaos, and Transport", Cambridge Univ. Press, Cambridge 1990.

[9] H. Löwe, W. Ehrfeld, V. Hessel, T. Richter and J. Schiewe, Proc. IMRET 4, Atlanta, USA, 2000, 31.

[10] V. Hessel, H. Löwe, C. Hofmann, F. Schönfeld, D. Wehle and B. Werner, Proc. IMRET 6, AIChE Pub. No. 164, New Orleans, USA, 2002, 39.

[11] F. Schönfeld, V. Hessel, and C. Hofmann, Lab on a Chip, in press.

[12] J.P. Boris, and D. L. Book, J. Comput. Phys., 11, 38 (1973).

[13] C.A. Fletcher, Computational Techniques for Fluid Dynamics; Springer-Verlag, Berlin (1991)

[14] S. Hardt and F. Schönfeld, AIChE J. 2003, 49, 578.